

Doubly charmed Ξ_{cc} molecular states from meson-baryon interaction

J. M. Dias,^{1,2,3,*} V. R. Debastiani,^{1,2,†} Ju-Jun Xie,^{1,‡} and E. Oset^{1,2,§}

¹*Institute of Modern Physics, Chinese Academy of Sciences, Lanzhou 730000, China*

²*Departamento de Física Teórica and IFIC,
Centro Mixto Universidad de Valencia-CSIC,
Institutos de Investigación de Paterna,
Aptdo. 22085, 46071 Valencia, Spain.*

³*Instituto de Física, Universidade de São Paulo,
C.P. 66318, 05389-970 São Paulo, SP, Brazil.*

Abstract

Stimulated by the new experimental LHCb findings associated with the Ω_c states, some of which we have described in a previous work as being dynamically generated through meson-baryon interaction, we have extended this approach to make predictions for new Ξ_{cc} molecular states in the $C = 2$, $S = 0$ and $I = 1/2$ sector. These states manifest themselves as poles in the solution of the Bethe-Salpeter equation in coupled channels. The kernels of this equation were obtained using the Lagrangians coming from the hidden local gauge symmetry, where the interactions are dominated by the exchange of light vector mesons. The extension of this approach to the heavy sector stems from the realization that the dominant interaction corresponds to having the heavy quarks as spectators, which implies the preservation of the heavy quark symmetry. As a result, we get several states: two states from the pseudoscalar meson-baryon interaction with $J^P = 1/2^-$, and masses around 4080 and 4090 MeV, and one at 4150 MeV for $J^P = 3/2^-$. Furthermore, from the vector meson-baryon interaction we get three states degenerate with $J^P = 1/2^-$ and $3/2^-$ from 4220 MeV to 4330 MeV, and two more states around 4280 MeV and 4410 MeV, degenerate with $J^P = 1/2^-$, $3/2^-$ and $5/2^-$.

PACS numbers: 14.40.Rt, 12.40.Yx, 13.75.Lb

* jdias@if.usp.br

† vinicius.rodrigues@ific.uv.es

‡ xiejujun@impcas.ac.cn

§ eulogio.oset@ific.uv.es

I. INTRODUCTION

Over the last decade, the field of hadron spectroscopy is living a new era due to a large bulk of experimental results, which has triggered an intense theoretical activity in order to describe and understand these experimental data. They are challenging our knowledge of hadron dynamics since many states cannot be accommodated within the standard picture for the hadron. In 2015, the LHCb reported the observation of the states $P_c^+(4380)$ and $P_c^+(4450)$ in the $J/\psi p$ invariant mass distribution [1–3] and, afterwards, five narrow Ω_c states [4] were measured in the $\Xi_c^+ K^-$ mass spectrum. Especially interesting was the observation of a doubly charmed baryon (DCB), called Ξ_{cc}^{++} , recently seen by the LHCb collaboration in the $\Lambda_c^+ K^- \pi^+ \pi^+$ final state, with mass around 3621 MeV [5]. This value is higher than that for the first doubly charmed state Ξ_{cc}^+ measured in the $\Lambda_c^+ K^- \pi^+$ mass spectrum, by SELEX in 2002 [6], and later confirmed in Ref. [7] by the same collaboration. However, this latter state was not confirmed by FOCUS [8], Belle [9], BABAR [10] and the LHCb [11] collaborations.

On the theoretical side, a DCB state with a mass similar to that one reported by the LHCb had been predicted in Ref. [12], using a renormalizable gauge field theory. A DCB was also predicted in Ref. [13], where the relativistic quark-diquark potential model was employed. Using the one gluon exchange model, the authors of Ref. [14] had also predicted a doubly heavy baryon state in which the mass value obtained is close to the one measured by the LHCb. In particular, these works advocate that the Ξ_{cc}^{++} should be accommodated in the quark picture. On the other hand, many other theoretical approaches were used to study doubly charmed baryon states¹ before the LHCb measurements, including even triply heavy baryons extended to the beauty sector [15].

More recently, in particular after the LHCb announcement of the newly Ξ_{cc}^{++} , a new wave of theoretical studies have aroused in an attempt to understand its properties, including also new predictions. In Ref. [17], the chiral corrections were employed to estimate the magnetic moments of DCB with $J = 1/2$. Weak decays were studied in Refs. [18, 19], strong and radiative decays were investigated in Ref. [20], and QCD sum rules were used in Ref. [21]. The molecular picture was also adopted. In Ref. [22], the meson-baryon transitions between the coupled channels $J/\psi N - \Lambda_c \bar{D}^{(*)} - \Sigma_c^{(*)} \bar{D}^{(*)}$ were constructed taking into account the pion

¹ We refer the reader to Ref. [16], which presents a review of the literature on those works.

and $D^{(*)}$ meson exchange, and then used as the potential in the complex scaled Schrödinger-type equation. According to their findings, if the $P_c(4380)$ exists as a hadronic molecular state, the existence of a $\Xi_{cc}^*(4380)$ with almost the same mass as the $P_c(4380)$ state should be expected. Studying the same type of interaction, that is, the meson-baryon one, in Ref. [23] an S -wave scattering of ground state doubly charmed baryons (Ξ_{cc}^{++} , Ξ_{cc}^+ , Ω_{cc}^+) and the light pseudoscalar (π , K , η) mesons was implemented by means of chiral effective theory, and several DCB resonances were predicted. This is particularly interesting and, since the LHCb has observed Ω_c resonances, we can expect there may exist Ξ_{cc} resonances as well. In view of this, in this work we study the meson-baryon interaction in order to investigate DCB resonances that can be confronted with the experimental measurements to be made in the near future.

Among the models employed to study meson-baryon interactions, one is particularly interesting and powerful to describe the meson-baryon interaction. It combines chiral dynamics with unitarity in coupled channels, named as chiral unitary approach. Using chiral Lagrangians we can obtain the transition amplitudes between all the relevant channels contributing to the interaction we are concerned. Then, these amplitudes are unitarized through the Bethe-Salpeter equation, from which bound states/resonances emerge as solutions in the complex energy plane. We say that these bound states/resonances are dynamically generated. One famous example was the long-standing two $\Lambda(1405)$ states [24–27].

The extension of the chiral unitary approach to describe vector meson-baryon interactions was done in Refs. [28, 29], where the authors used the Lagrangians from the hidden gauge approach [30–32], which extends the chiral Lagrangians to include vector mesons. Its extension to the charm sector was done in Refs. [33–36]. In particular, in Refs. [33, 34] it was found that in the dominant terms of the interaction the heavy quarks are spectators and, hence, the dominant contributions come from the exchange of light vector mesons. As a consequence, this approach satisfies the heavy quark spin symmetry, which is the symmetry of QCD that says the interaction is independent of the spin of the heavy quarks in the limit of the heavy quark mass going to infinity.

In Ref. [37], we have done such an extension of the hidden gauge to the charm sector taking into account the spin-flavor wave function for baryons and, since the heavy quarks act as spectators, the vector-baryon-baryon (VBB) vertex for the diagonal terms was obtained using the $SU(3)$ content of $SU(4)$. The work shares many elements and similar results

with the work of Ref. [38], where baryon wave functions within $SU(4)$ are strictly used. A different approach motivated by the works of Refs. [37–39] is done in Ref. [40], where some states obtained are also associated with the observed states. In particular, this was done after reviewing the renormalization scheme of Ref. [39], where some Ω_c states had been predicted with masses smaller than the ones observed by the LHCb.

Following the approach of Ref. [37], we have described some of the Ω_c states observed by the LHCb collaboration. A remarkable agreement with the experimental results for those singly charmed baryon states were obtained. For $J^P = 1/2^-$ two states can be related to the observed ones, the $\Omega_c(3090)$ and $\Omega_c(3050)$. In addition, another pole with $J^P = 3/2^-$ could be related to the $\Omega_c(3119)$. Motivated by this remarkable agreement, we have also employed the same approach, but this time to predict singly heavy baryon resonances in the beauty sector [41], named as Ω_b states. In view of this, and stimulated by the LHCb recent discovery of a doubly charmed baryon structure, Ξ_{cc}^{++} , we have used this same approach in order to investigate DCB states, that can be dynamically generated through the interaction between doubly and singly charmed baryon with pseudoscalar and vector mesons with or without charm.

The planned experiments, for instance, like the one at the FAIR facility will involve studies of charm physics, and the observation of such new states, certainly will shed light on the debate about their quantum numbers, production mechanism and quark content. This will certainly be a good scenario to test most of the models which are used to understand those states from the multiquark point of view.

II. THEORETICAL FRAMEWORK

In order to obtain the transition matrix elements using the Bethe-Salpeter equation, we must write down the relevant space of states in the $C = 2$, $S = 0$ and $I = 1/2$ sector, which are the channels contributing to the meson-baryon interaction in S -wave we are concerned with. We use the channels established in Ref. [39] and separate them into different cases from the interaction of baryons ($J^P = 1/2^+$, $3/2^+$) with pseudoscalar (0^-) and vector mesons (1^-), as it was done in Ref. [37] for the case of the Ω_c states. We should emphasize here that the channels listed in Ref. [39] were written taking into account the previous value for the Ξ_{cc} mass which was 3519 MeV. In this work we are considering the same channels of

Ref. [39] but using the value reported by the LHCb collaboration [5], which is equal to 3621 MeV. This means we are considering this new value as the ground state for the Ξ_{cc} baryon. Accordingly, we also update the estimate for the excited Ξ_{cc}^* , taking its mass as 81 MeV higher than that of Ξ_{cc} , similar to the $\Xi'_c - \Xi_c^*$ mass splitting, as done in Ref. [39]. The estimates for the Ω_{cc} and Ω_{cc}^* masses are also taken as the same adopted in Ref. [39], given in Ref. [42]. The other masses are taken as isospin averages of the ones listed by the Particle Data Group [43]. In Tables I, II, III and IV we show the channels and their respective thresholds reevaluated taking $M_{\Xi_{cc}} = 3621$ MeV.

TABLE I. Baryon-pseudoscalar states ($J^P = 1/2^-$) chosen and threshold mass in MeV.

Channel	$\Xi_{cc}\pi$	$\Lambda_c D$	$\Xi_{cc}\eta$	$\Omega_{cc}K$	$\Sigma_c D$	$\Xi_c D_s$	$\Xi'_c D_s$
Threshold	3759	4154	4169	4208	4321	4438	4545

TABLE II. Baryon-pseudoscalar states ($J^P = 3/2^-$) chosen and threshold mass in MeV.

Channel	$\Xi_{cc}^*\pi$	$\Xi_{cc}^*\eta$	Ω_{cc}^*K	$\Sigma_c^* D$	$\Xi_c^* D_s$
Threshold	3840	4250	4291	4385	4615

TABLE III. Baryon-vector meson states ($J^P = 1/2^-, 3/2^-$) chosen and threshold mass in MeV.

Channel	$\Lambda_c D^*$	$\Xi_{cc}\rho$	$\Xi_{cc}\omega$	$\Sigma_c D^*$	$\Xi_c D_s^*$	$\Omega_{cc} K^*$	$\Xi_{cc}\phi$	$\Xi'_c D_s^*$
Threshold	4295	4397	4404	4462	4582	4606	4641	4689

TABLE IV. Baryon-vector meson states ($J^P = 1/2^-, 3/2^-, 5/2^-$) chosen and threshold mass in MeV.

Channel	$\Xi_{cc}^*\rho$	$\Xi_{cc}^*\omega$	$\Sigma_c^* D^*$	$\Omega_{cc}^* K^*$	$\Xi_{cc}^*\phi$	$\Xi_c^* D_s^*$
Threshold	4478	4485	4526	4689	4722	4759

Next, we will discuss the use of Lagrangians from hidden local gauge symmetry which provide an easy manner to evaluate the meson-baryon interaction involving the channels listed in Tables I, II, III and IV.

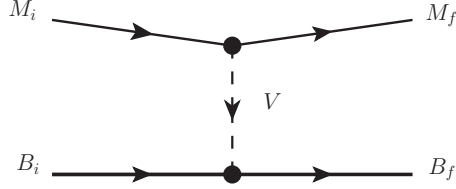


FIG. 1. Diagram representing the meson-baryon interaction through vector meson exchange. $M_i(M_f)$ and $B_i(B_f)$ are the initial (final) meson and baryon states, respectively, taking place on the interaction, while V stands for the vector meson exchanged.

A. Transition amplitudes

The use of chiral Lagrangians to calculate the transition amplitudes is complicated when states in the charm sector are involved. This happens because one needs to extend those Lagrangians from $SU(3)$ to $SU(4)$ and the use of this latter symmetry must be handled with care when dealing with mesons and baryons with such disparate masses. On the other hand, the use of the Lagrangians coming from the hidden local gauge symmetry allows us to make use of the $SU(3)$ content of $SU(4)$ since the heavy quark is treated as a spectator in our formalism. As a consequence the rules of heavy quark spin symmetry are fulfilled [44] for the dominant diagonal interactions.

In the local hidden gauge approach in $SU(3)$, the meson-baryon interaction proceeds by means of vector meson exchange as illustrated in Fig. 1. According to the hidden local gauge approach, the vector-pseudoscalar-pseudoscalar coupling (VPP), i. e. the upper vertex of the diagram depicted in Fig. 1 is described by the following Lagrangian

$$\mathcal{L}_{VPP} = -ig \langle [\phi, \partial_\mu \phi] V^\mu \rangle, \quad (1)$$

where ϕ and V^μ are the $SU(3)$ matrices for pseudoscalar and vector mesons, respectively, given by

$$\phi = \begin{pmatrix} \frac{1}{\sqrt{2}}\pi^0 + \frac{1}{\sqrt{6}}\eta & \pi^+ & K^+ \\ \pi^- & -\frac{1}{\sqrt{2}}\pi^0 + \frac{1}{\sqrt{6}}\eta & K^0 \\ K^- & \bar{K}^0 & -\frac{2}{\sqrt{6}}\eta \end{pmatrix}, \quad (2)$$

and

$$V_\mu = \begin{pmatrix} \frac{\rho^0}{\sqrt{2}} + \frac{\omega}{\sqrt{2}} & \rho^+ & K^{*+} \\ \rho^- & -\frac{\rho^0}{\sqrt{2}} + \frac{\omega}{\sqrt{2}} & K^{*0} \\ K^{*-} & \bar{K}^{*0} & \phi \end{pmatrix}_\mu, \quad (3)$$

while the symbol $\langle \dots \rangle$ in Eq. (1) stands for the $SU(3)$ trace and the coupling $g = M_V/2f_\pi$, with $f_\pi = 93$ MeV being the pion decay constant. The extension of Eq. (1) to $SU(4)$ is straightforward and the discussion on how to do this can be found in Refs. [33, 34]. Alternatively one can use an explicit method, rather clarifying in the case of exchange of light vector mesons, which leaves the heavy quarks as spectators, consisting in explicitly writing the operators for vector exchange in terms of quarks. This is done in Ref. [45] and the conclusion is that one can use directly Eq. (1) with $SU(4)$ matrices for ϕ and V_μ [33, 34] and the procedure projects automatically in $SU(3)$ in the case that the heavy quarks are spectators.

On the other hand, the vector-baryon-baryon (VBB) in $SU(3)$, can be calculated within the local hidden gauge formalism using the following Lagrangian,

$$\mathcal{L}_{VBB} = g \left(\langle \bar{B} \gamma_\mu [V^\mu, B] \rangle + \langle \bar{B} \gamma_\mu B \rangle \langle V^\mu \rangle \right), \quad (4)$$

with B associated with the $SU(3)$ matrix for the baryon octet, which is

$$B = \begin{pmatrix} \frac{1}{\sqrt{2}}\Sigma^0 + \frac{1}{\sqrt{6}}\Lambda & \Sigma^+ & p \\ \Sigma^- & -\frac{1}{\sqrt{2}}\Sigma^0 + \frac{1}{\sqrt{6}}\Lambda & n \\ \Xi^- & \Xi^0 & -\frac{2}{\sqrt{6}}\Lambda \end{pmatrix}. \quad (5)$$

Unlike Eq. (1), the $SU(4)$ extension of Eq. (4) is not trivial. However, in this work we follow the procedure adopted in Refs. [37, 41], which allows us to obtain in an easy manner the VBB vertex without making use of $SU(4)$. In order to do this, we write the vector meson exchanged and the baryon in terms of quarks. For instance, let us consider that we have for the VBB vertex a ρ meson and two protons, that is the ρpp vertex. The ρ^0 meson wave function in terms of quarks is given by

$$\rho^0 = \frac{1}{\sqrt{2}}(u\bar{u} - d\bar{d}). \quad (6)$$

Inherent in the approach of Refs. [37–39] is the neglect of the three momenta of the particles compared to the vector meson mass. This allows us to make the approximation $\gamma_\mu \rightarrow \gamma_0$, and

hence applying Eq. (6) in the proton wave function as a number operator with a coupling g provides us a spin independent operator at the quark level. In addition, we know that the proton wave function can be written as

$$p = \frac{1}{\sqrt{2}}|\phi_{MS}\chi_{MS} + \phi_{MA}\chi_{MA}\rangle, \quad (7)$$

where $\phi_{MS(MA)}$ and $\chi_{MS(MA)}$ are the flavor and spin mixed symmetric (antisymmetric) wave functions, respectively. Therefore, for the ρpp vertex we have

$$\langle p|g\rho|p\rangle = \frac{g}{2}\langle\phi_{MS}\chi_{MS} + \phi_{MA}\chi_{MA}|\frac{1}{\sqrt{2}}(u\bar{u} - d\bar{d})|\phi_{MS}\chi_{MS} + \phi_{MA}\chi_{MA}\rangle, \quad (8)$$

which provides us the same result as if we had used Eq. (4). We use this method to evaluate the coupling of the vectors with baryons in the charm sector.

B. Baryon wave functions

In this subsection, we are going to write the baryon wave functions, which will be useful to evaluate the VBB vertex. In order to obtain this vertex through the method we have discussed previously, where we have used the ρpp vertex as an example, we have to write down the spin-flavor wave functions for the baryons with $J^P = 1/2^+$ and $J^P = 3/2^+$. The spin-flavor wave functions associated with all of them are displayed in Tables V and VI. In those tables, the flavor part of the wave function is explicitly written leaving the heavy quarks as spectators and using $SU(3)$ symmetry in the light quarks, where the $SU(3)$ content can be mixed symmetric or mixed antisymmetric, $\phi_{MS(MA)}$, while the spin part, can be mixed symmetric, antisymmetric $\chi_{MS(MA)}$, or fully symmetric, χ_S , as defined in the last column.

Once we know the spin-flavor wave functions for the baryons, we can obtain the VBB vertex, which corresponds to the lower one in Fig. 1. For instance, if a Ξ_{cc} is involved in a given transition, using its corresponding wave function defined in Table V, we can obtain the $\Xi_{cc}^{++}\Xi_{cc}^{++}\rho^0$ vertex evaluating the $\langle\Xi_{cc}^{++}|g\rho^0|\Xi_{cc}^{++}\rangle$ matrix element, which is

$$\begin{aligned} \langle\Xi_{cc}^{++}|g\rho^0|\Xi_{cc}^{++}\rangle &= g\langle ccu|\otimes\langle\chi_{MS}|\left[\frac{1}{\sqrt{2}}(u\bar{u} - d\bar{d})\right]|\chi_{MS}\rangle\otimes|ccu\rangle \\ &= \frac{g}{\sqrt{2}}. \end{aligned} \quad (9)$$

Analogously, for all the remaining VBB vertices we are concerned, we will follow this procedure.

TABLE V. Wave functions for baryon with $J^P = 1/2^+$.

States	I, J	Flavor	Spin ($S_z = 1/2$)
Λ_c	0, 1/2	$\frac{c}{\sqrt{2}}(ud - du)$	$\frac{\uparrow}{\sqrt{2}}(\uparrow\downarrow - \downarrow\uparrow)$ χ_{MA}^a
Σ_c^+	1, 1/2	$\frac{c}{\sqrt{2}}(ud + du)$	$\frac{1}{\sqrt{6}}(\uparrow\uparrow\uparrow + \downarrow\uparrow\uparrow - 2\uparrow\uparrow\downarrow)$ χ_{MS}^b
Ξ_c^+	1/2, 1/2	$\frac{c}{\sqrt{2}}(us - su)$	$\frac{\uparrow}{\sqrt{2}}(\uparrow\downarrow - \downarrow\uparrow)$ χ_{MA}
$\Xi_c'^+$	1/2, 1/2	$\frac{c}{\sqrt{2}}(us + su)$	χ_{MS}
Ξ_{cc}^{++}	1/2, 1/2	ccu	χ_{MS}
Ω_{cc}	0, 1/2	ccs	χ_{MS}

^a Mixed antisymmetric

^b Mixed symmetric

 TABLE VI. Wave functions for baryon with $J^P = 3/2^+$.

States	I, J	Flavor	Spin ($S_z = 3/2$)
Σ_c^{*+}	1, 3/2	$\frac{c}{\sqrt{2}}(ud + du)$	$\uparrow\uparrow\uparrow$ χ_S^a
Ξ_c^{*+}	1/2, 3/2	$\frac{c}{\sqrt{2}}(us + su)$	χ_S
Ω_{cc}^*	1/2, 3/2	ccs	χ_S

^a Fully symmetric

In order to match the Ξ_{cc} isospin, we should construct states with $I = 1/2$. We have the following multiplets

$$\begin{aligned}
 \Xi_{cc} &= \begin{pmatrix} \Xi_{cc}^{++} \\ \Xi_{cc}^+ \end{pmatrix}; \quad \Xi_c = \begin{pmatrix} \Xi_c^+ \\ \Xi_c^0 \end{pmatrix}; \quad \Xi_c' = \begin{pmatrix} \Xi_c'^+ \\ \Xi_c'^0 \end{pmatrix}; \quad \Sigma_c = \begin{pmatrix} -\Sigma_c^{++} \\ \Sigma_c^+ \\ \Sigma_c^0 \end{pmatrix}; \\
 D &= \begin{pmatrix} D^+ \\ -D^0 \end{pmatrix}; \quad K = \begin{pmatrix} K^+ \\ K^0 \end{pmatrix}; \quad \pi = \begin{pmatrix} -\pi^+ \\ \pi^0 \\ \pi^- \end{pmatrix}, \quad (10)
 \end{aligned}$$

from which we can obtain the $I = 1/2$ states.

Now, we have all the elements needed to evaluate the transition amplitudes, depicted generically in Fig. 1, between the relevant channels listed in Tables I, II, III and IV for each J^P case. For $PB \rightarrow PB$ transitions by means of vector meson exchange, two vertices must

be calculated. They are the VPP , that can be obtained from the Lagrangian defined in Eq. (1), and the VBB , which is obtained employing the method we have just discussed. On the other hand, for $VB \rightarrow VB$ transitions the only difference is that now we have the VVV vertex instead of VPP one, and it can be evaluated using the following Lagrangian

$$\mathcal{L}_{VVV} = ig \langle [V^\mu, \partial_\nu V_\mu] V^\nu \rangle, \quad (11)$$

with the coupling g the same as in Eq. (1). In the case where the three-momentum of the vector meson is neglected versus the vector meson mass, as we also do here, only $\nu = 0$ contributes in Eq. (11) which forces V^ν to be the exchanged vector, and the structure of the vertex is identical to the one of Eq. (1) for pseudoscalars, with the additional factor $\vec{\epsilon} \cdot \vec{\epsilon}'$, with $\vec{\epsilon}, \vec{\epsilon}'$ the polarization vectors of the external vector mesons [28]. Following this procedure we can calculate all the transition amplitudes (see Appendix A for more details), which have the same structure for every transition we are considering in this work, which is

$$V_{ij} = C_{ij} \frac{1}{4f_\pi^2} (p^0 + p'^0), \quad (12)$$

where p^0 and p'^0 are the energies of the incoming and outgoing mesons, while the C_{ij} are the coefficients, given in Table VII, for the pseudoscalar meson-baryon case with $J^P = 1/2^-$. Furthermore, the indices i, j stand for the initial and final channels, respectively. For the vector meson-baryon, the coefficients are given in Table VIII. The other cases are tabulated in Tables IX and X, respectively. Alternatively, we can also use the expression below

$$V_{ij} = C_{ij} \frac{2\sqrt{s} - M_{B_i} - M_{B_j}}{4f_\pi^2} \sqrt{\frac{M_{B_i} + E_{B_i}}{2M_{B_i}}} \sqrt{\frac{M_{B_j} + E_{B_j}}{2M_{B_j}}}, \quad (13)$$

which is obtained, according to Ref. [46], when we take into account relativistic corrections in S -wave.

C. The scattering matrix for meson-baryon interaction

In order to unitarize the transition amplitudes, often called potentials, given by Eqs. (12) or (13), we have to use them as the kernel of the Bethe-Salpeter equation, where poles in resulting scattering matrices correspond to bound states or resonances. The Bethe-Salpeter equation in its on-shell factorization form [24, 47, 48] is defined as

$$T = (1 - VG)^{-1} V, \quad (14)$$

TABLE VII. C_{ij} coefficients of Eq. (12) for the pseudoscalar meson-baryon states coupling to $J^P = 1/2^-$ in S -wave.

$PB_{1/2}$	$\Xi_{cc}\pi$	$\Lambda_c D$	$\Xi_{cc}\eta$	$\Omega_{cc}K$	$\Sigma_c D$	$\Xi_c D_s$	$\Xi'_c D_s$
$\Xi_{cc}\pi$	$-\frac{4}{3}$	0	$-\frac{\sqrt{2}}{3}$	$-\sqrt{\frac{3}{2}}$	0	0	0
$\Lambda_c D$		-1	0	0	0	-1	0
$\Xi_{cc}\eta$			0	$-\frac{1}{\sqrt{3}}$	0	0	0
$\Omega_{cc}K$				-1	0	0	0
$\Sigma_c D$					-3	0	$-\frac{1}{\sqrt{3}}$
$\Xi_c D_s$						-1	0
$\Xi'_c D_s$							-1

TABLE VIII. C_{ij} coefficients of Eq. (12) for the vector meson-baryon states coupling to $J^P = 1/2^-, 3/2^-$ in S -wave.

$VB_{1/2}$	$\Lambda_c D^*$	$\Xi_{cc}\rho$	$\Xi_{cc}\omega$	$\Sigma_c D^*$	$\Xi_c D_s^*$	$\Omega_{cc}K^*$	$\Xi_{cc}\phi$	$\Xi'_c D_s^*$
$\Lambda_c D^*$	-1	0	0	0	-1	0	0	0
$\Xi_{cc}\rho$		$-\frac{4}{3}$	$-\frac{1}{\sqrt{3}}$	0	0	$-\sqrt{\frac{3}{2}}$	0	0
$\Xi_{cc}\omega$			0	0	0	$-\frac{1}{\sqrt{2}}$	0	0
$\Sigma_c D^*$				-3	0	0	0	$-\frac{1}{\sqrt{3}}$
$\Xi_c D_s^*$					-1	0	0	0
$\Omega_{cc}K^*$						-1	1	0
$\Xi_{cc}\phi$							0	0
$\Xi'_c D_s^*$								-1

where V is the matrix that describes the transition amplitudes between each channel listed in Tables I, II, III and IV. G is the meson-baryon loop function, which is divergent. It is possible to evaluate this function by means of dimensional regularization or with a three momentum cutoff. In this work, we use the cutoff method since the dimensional regularization in the heavy sector might lead to solutions that are not related to physical states [49]. This happens because in that scheme of regularization the loop function can assume positive values below threshold. As a result, poles might manifest in the solution even with the potential being

TABLE IX. C_{ij} coefficients of Eq. (12) for the pseudoscalar meson-baryon states coupling to $J^P = 3/2^-$ in S -wave.

$PB_{3/2}$	$\Xi_{cc}^*\pi$	$\Xi_{cc}^*\eta$	Ω_{cc}^*K	Σ_c^*D	$\Xi_c^*D_s$
$\Xi_{cc}^*\pi$	$-\frac{4}{3}$	$-\frac{\sqrt{2}}{3}$	$-\sqrt{\frac{3}{2}}$	0	0
$\Xi_{cc}^*\eta$		0	$-\frac{1}{\sqrt{3}}$	0	0
Ω_{cc}^*K			-1	0	0
Σ_c^*D				-3	$-\frac{1}{\sqrt{3}}$
$\Xi_c^*D_s$					-1

TABLE X. C_{ij} coefficients of Eq. (12) for the vector meson-baryon states coupling to $J^P = 1/2^-, 3/2^-, 5/2^-$ in S -wave.

$VB_{3/2}$	$\Xi_{cc}^*\rho$	$\Xi_{cc}^*\omega$	$\Sigma_c^*D^*$	$\Omega_{cc}^*K^*$	$\Xi_{cc}^*\phi$	$\Xi_c^*D_s^*$
$\Xi_{cc}^*\rho$	$-\frac{4}{3}$	$-\frac{1}{\sqrt{3}}$	0	$-\sqrt{\frac{3}{2}}$	0	0
$\Xi_{cc}^*\omega$		0	0	$-\frac{1}{\sqrt{2}}$	0	0
$\Sigma_c^*D^*$			-3	0	0	$-\frac{1}{\sqrt{3}}$
$\Omega_{cc}^*K^*$				-1	1	0
$\Xi_{cc}^*\phi$					0	0
$\Xi_c^*D_s^*$						-1

repulsive. In the cutoff method the meson-baryon loop function is given by

$$\begin{aligned}
G_l &= i \int \frac{d^4q}{(2\pi)^4} \frac{M_l}{E_l(\mathbf{q})} \frac{1}{k^0 + p^0 - q^0 - E_l(\mathbf{q}) + i\epsilon} \frac{1}{\mathbf{q}^2 - m_l^2 + i\epsilon} \\
&= \int_{|\mathbf{q}| < q_{max}} \frac{d^3\mathbf{q}}{(2\pi)^3} \frac{1}{2\omega_l(\mathbf{q})} \frac{M_l}{E_l(\mathbf{q})} \frac{1}{k^0 + p^0 - \omega_l(\mathbf{q}) - E_l(\mathbf{q}) + i\epsilon}, \tag{15}
\end{aligned}$$

where the subscript l is the label for the l th-channel, while $k^0 + p^0 = \sqrt{s}$ and ω_l, E_l stand for the meson and baryon energies, respectively. In the next section, we show the results for $q_{max} = 650$ MeV, which is the same value used in previous works [37, 41], where the same framework discussed here was applied to investigate meson-baryon interactions in the heavy sector. It was shown in Refs. [50, 51] that the same value of cutoff has to be used for all channels in order to respect the rules of heavy quark symmetry.

The bound states and resonances can be associated to the poles that are solutions of

the Bethe-Salpeter equation, defined in Eq. (14). In order to look for these poles we need to obtain the T -matrix in the complex energy plane, for which we have calculated the meson-baryon G function in the first (I) and second (II) Riemann sheet [47]. This is done by changing G in Eq. (14) to G^{II} in order to obtain T^{II} . The loop G^{II} is the analytic continuation of the loop function in the second Riemann sheet, and it is given by

$$G_l^{II}(\sqrt{s}) = G_l^I(\sqrt{s}) + i \frac{M_l}{2\pi\sqrt{s}} p, \text{ with } \text{Im}(p) > 0, \\ p = \frac{\lambda^{1/2}(s, m_l^2, M_l^2)}{2\sqrt{s}}, \quad (16)$$

with m_l and M_l being the meson and baryon masses of the l -channel, respectively, while G^I (given by Eq. (15)) and G_l^{II} stand for the loop function in the first and second Riemann sheet, respectively. In Eq. (16), we use G_l^{II} when the l th-channel is open, i. e. $\text{Re}(\sqrt{s}) > m_l + M_l$. On the other hand, when the channel is closed, that is $\text{Re}(\sqrt{s}) < m_l + M_l$, we have $G_l^{II} = G_l^I$.

It is also possible to evaluate the couplings g_l of the state to the different meson-baryon channels. In order to do this, note that close to the pole the amplitude in the complex plane for a diagonal transition can be written as

$$T_u(s) \approx \frac{g_l^2}{\sqrt{s} - z_R}, \quad (17)$$

where $z_R = M_R + i\Gamma_R/2$ stands for the position of the bound state/resonance [52]. Hence, the coupling can be evaluated as the residue at the pole of $T_u(s)$, by means of the following formula

$$g_l^2 = \frac{r}{2\pi} \int_0^{2\pi} T_u(z(\theta)) e^{i\theta} d\theta, \quad (18)$$

where $z = z_R + r e^{i\theta}$.

In addition, with the coupling constant and the G function calculated at the pole, we can obtain $g_l G_l(z_R)$, which is proportional to the wave function at the origin in the l th-channel [53].

III. RESULTS

In Table XI we show the poles we have found according to the procedure discussed previously. They are related to the interaction involving a pseudoscalar meson and $1/2^+$ baryon in S -wave, such that for this case we have poles associated to the $J^P = 1/2^-$ quantum

numbers. In addition, we also show the couplings of these states to the channels spanning the space of states listed in Table I as well as the product $g_l G_l^{II}$, with G_l^{II} being the loop function evaluated at the pole in the second Riemann sheet. We get two states separated approximately by ≈ 10 MeV, with one at 4082.79 MeV and the other at 4092.20 MeV. From the results obtained for the couplings as well as for the wave function at the origin, we observe that the first pole couples strongly to the $\Sigma_c D$ channel. It also couples to $\Xi'_c D_s$, but with a smaller value than to the former channel. We can understand this by looking at Table VII. According to that table only the $\Sigma_c D \rightarrow \Sigma_c D$ and $\Sigma_c D \rightarrow \Xi'_c D_s$ transitions are allowed, with the coefficient related to the diagonal one as the biggest value. Therefore, we can say that this pole is mostly a $\Sigma_c D$ molecule. For the second pole, at 4092.20 MeV, we

TABLE XI. Poles and couplings in the $PB_{1/2}$, $J^P = 1/2^-$ sector, with $q_{max} = 650$ MeV, and $g_l G_l^{II}$ in MeV.

4082.79	$\Xi_{cc}\pi$	$\Lambda_c D$	$\Xi_{cc}\eta$	$\Omega_{cc}K$	$\Sigma_c D$	$\Xi_c D_s$	$\Xi'_c D_s$
g_l	0	0	0	0	8.86	0	1.93
$g_l G_l^{II}$	0	0	0	0	-31.29	0	-4.04
4092.20	$\Xi_{cc}\pi$	$\Lambda_c D$	$\Xi_{cc}\eta$	$\Omega_{cc}K$	$\Sigma_c D$	$\Xi_c D_s$	$\Xi'_c D_s$
g_l	0	4.01	0	0	0	3.75	0
$g_l G_l^{II}$	0	-29.49	0	0	0	-9.76	0

see that it couples to both $\Lambda_c D$ and $\Xi_c D_s$ channels with almost the same magnitude. The only open channel for both states found is $\Xi_{cc}\pi$, but as can be seen from Table XI, they do not couple to this channel.

TABLE XII. Poles and couplings in the $PB_{3/2}$, $J^P = 3/2^-$ sector, with $q_{max} = 650$ MeV, and $g_l G_l^{II}$ in MeV.

4149.67	$\Xi_{cc}^*\pi$	$\Xi_{cc}^*\eta$	Ω_{cc}^*K	$\Sigma_c^* D$	$\Xi_c^* D_s$
g_l	0	0	0	8.82	1.30
$g_l G_l^{II}$	0	0	0	-31.46	-2.71

The results associated with the interaction involving a pseudoscalar meson and a baryon with $J^P = 3/2^+$ in S -wave, are displayed in Table XII. Analogously to the previous case, we

also present the couplings together with the wave function at the origin, that is the $g_l G_l^{II}$ product. In this case, we have just one pole at 4149.67 MeV, coupling mostly to $\Sigma_c^* D$ and with less intensity to the $\Xi_c^* D_s$ channel. As can be seen looking at the Table III for the thresholds, only the $\Xi_{cc}^* \pi$ channel is open. The coupling to $\Sigma_c^* D$ is almost seven times bigger than the value for the other channel, $\Xi_c^* D_s$, then this pole is naturally associated with a $\Sigma_c^* D$ molecule. This pole would be the spin partner of the pole found at 4082.79 MeV from the pseudoscalar-baryon (PB) interaction, with $J^P = 1/2^-$.

Next we look for the states with degenerate $J^P = 1/2^-, 3/2^-$, resulting from the interaction in S -wave of vector mesons and baryons with $J^P = 1/2^+$. Our findings for this particular case can be seen in Table XIII. Three states have been found, at 4217.21 MeV, 4229.19 MeV and at 4328.65 MeV. The first of them couples strongly to $\Sigma_c D^*$ and little to the $\Xi_c' D_s^*$ channel, and hence, this pole qualifies as a $\Sigma_c D^*$ bound state. The second state found, at 4229.19 MeV, couples to both $\Lambda_c D^*$ and $\Xi_c D_s^*$ with similar values for the couplings, however, when we compare the values for the product $g_l G_l^{II}$, we see that the one for the $\Lambda_c D^*$ channel is much bigger than that for $\Xi_c D_s^*$. The same behavior is found for the last pole, at 4328.65 MeV, whose couplings to $\Xi_{cc} \rho$ and to $\Omega_{cc} K^*$ are of the same order, while the value for the wave function at the origin for the former channel is bigger than that for the latter one. It is worth mentioning that three states were also obtained in the same $VB_{1/2}$, $J^P = 1/2^-, 3/2^-$ sector for the Ω_c and Ω_b states, respectively, studied in Refs. [37, 41]. We note that for the first and second poles at 4217.21 MeV and 4229.19 MeV, all channels are closed for decay. The third pole at 4328.65 MeV has about 30 MeV of phase space to decay into $\Lambda_c D^*$, however in our approach it does not couple to this channel since it would require the exchange of a heavy vector meson.

Finally we also show in Table XIV the results for the vector meson-baryon states, with $J^P = 3/2^+$ for the baryon. In this case, we obtain two poles: 4280.43 MeV and 4409.61 MeV. The first one couples strongly to $\Sigma_c^* D^*$ and since its coupling to the other channel, $\Xi_c^* D_s^*$, is four times smaller than the first one, this pole is likely a $\Sigma_c^* D^*$ molecule. On the other hand, the second pole couples almost to all channels, except for the $\Sigma_c^* D^*$ and $\Xi_c^* D_s^*$. It couples with similar values for the coupling to the channels: $\Xi_{cc}^* \rho$ and $\Omega_{cc}^* K^*$; and next to $\Xi_{cc}^* \omega$, and a little to $\Xi_{cc}^* \phi$. But, by looking at the wave function at the origin we conclude that this last pole comes mostly from the $\Xi_{cc}^* \rho$ channel.

Evidence of three resonances at higher energies has also been found. In the $B_{1/2} P$ sector

TABLE XIII. Poles and couplings in the $VB_{1/2}$, $J^P = 1/2^-, 3/2^-$ sector, with $q_{max} = 650$ MeV, and $g_l G_l^{II}$ in MeV.

4217.21	$\Lambda_c D^*$	$\Xi_{cc}\rho$	$\Xi_{cc}\omega$	$\Sigma_c D^*$	$\Xi_c D_s^*$	$\Omega_{cc} K^*$	$\Xi_{cc}\phi$	$\Xi'_c D_s^*$
g_l	0	0	0	9.31	0	0	0	2.03
$g_l G_l^{II}$	0	0	0	-30.40	0	0	0	-3.94
4229.19	$\Lambda_c D^*$	$\Xi_{cc}\rho$	$\Xi_{cc}\omega$	$\Sigma_c D^*$	$\Xi_c D_s^*$	$\Omega_{cc} K^*$	$\Xi_{cc}\phi$	$\Xi'_c D_s^*$
g_l	4.21	0	0	0	3.98	0	0	0
$g_l G_l^{II}$	-28.70	0	0	0	-9.59	0	0	0
4328.65	$\Lambda_c D^*$	$\Xi_{cc}\rho$	$\Xi_{cc}\omega$	$\Sigma_c D^*$	$\Xi_c D_s^*$	$\Omega_{cc} K^*$	$\Xi_{cc}\phi$	$\Xi'_c D_s^*$
g_l	0	2.95	1.23	0	0	2.66	-0.56	0
$g_l G_l^{II}$	0	-35.46	-14.21	0	0	-14.72	2.64	0

TABLE XIV. Poles and couplings in the $VB_{3/2}$, $J^P = 1/2^-, 3/2^-, 5/2^-$ sector, with $q_{max} = 650$ MeV, and $g_l G_l^{II}$ in MeV.

4280.43	$\Xi_{cc}^* \rho$	$\Xi_{cc}^* \omega$	$\Sigma_c^* D^*$	$\Omega_{cc}^* K^*$	$\Xi_{cc}^* \phi$	$\Xi_c^* D_s^*$
g_l	0	0	9.31	0	0	2.03
$g_l G_l^{II}$	0	0	-30.42	0	0	-3.90
4409.61	$\Xi_{cc}^* \rho$	$\Xi_{cc}^* \omega$	$\Sigma_c^* D^*$	$\Omega_{cc}^* K^*$	$\Xi_{cc}^* \phi$	$\Xi_c^* D_s^*$
g_l	2.95	1.23	0	2.65	-0.56	0
$g_l G_l^{II}$	-35.51	-14.22	0	-14.63	2.62	0

a state coupling mostly to $\Xi'_c D_s$ was found around 4520 MeV. This state also couples to $\Sigma_c D$, and would be the “heavy partner” of the pole found around 4080 MeV. However, the pole is close to the threshold of $\Xi'_c D_s$, which is about 200 MeV above the one of $\Sigma_c D$. At this energy the propagator of $\Sigma_c D$ is already too far from its threshold and its real part becomes positive, what can affect the unitarization of the amplitude and yield unreliable results. The same happens in the $B_{1/2} P$ sector, where a state coupling mostly to $\Xi_c^* D_s$, and also to $\Sigma_c^* D$, was found around 4575 MeV; and in the $B_{1/2} V$ sector, where a state coupling mostly to $\Xi'_c D_s^*$, and also to $\Sigma_c D^*$, was found around 4660 MeV. In order to be sure these poles have physical meaning and do not come from the influence of the lower channel, we

have repeated the calculation using only the single dominant channel ($\Xi'_c D_s$, $\Xi_c^* D_s$ and $\Xi'_c D_s^*$, respectively) and we have found that the resonances are still present moving 10 MeV or less from the previous pole position. Therefore, these poles have indeed physical meaning; the only difference is that their pole position has larger uncertainties in comparison with the results presented in Tables [XI](#), [XII](#), [XIII](#) and [XIV](#).

IV. CONCLUSIONS

Using a framework employed to study the Ω_c states, recently observed by the LHCb collaboration, and also used to predict similar structures in the beauty sector, named as Ω_b states, which are dynamically generated through meson-baryon interaction, we have investigated the dynamical generation of possible doubly charmed heavy baryons resonances in the $C = 2$, $S = 0$ and $I = 1/2$ sector. In particular, the transition amplitudes between the relevant channels are inspired in the Lagrangians from the hidden local gauge approach. In order to deal with the VBB vertex, the spin-flavor wave functions for the baryons were constructed considering the heavy quarks as spectators, allowing us to extend the VBB interaction to the heavy sector in an easy manner, using the $SU(3)$ content of $SU(4)$.

These transition amplitudes are unitarized taking them as the kernel of the Bethe-Salpeter equation, whose solutions can be associated with physical states. Using this approach, we have just one parameter, which is the regulator in the loop function of the meson-baryon states. We have used the cutoff regularization method with the same cutoff used in previous works in which we have employed this method to study other meson-baryon interactions in the beauty sector as well as to study singly charmed baryon resonances, recently observed by the LHCb and called Ω_c states.

We obtain two poles, one at 4083 MeV and at 4092 MeV, for pseudoscalar meson-baryon interaction with $J^P = 1/2^-$, and another one at 4150 MeV for $J^P = 3/2^-$ quantum numbers. Furthermore, we have also considered the degenerate cases, stemming from the interaction of vector meson-baryon, that provides three states with $J^P = 1/2^-$ and $3/2^-$: at 4217 MeV, 4229 MeV and 4329 MeV, and two more with $J^P = 1/2^-$, $3/2^-$ and $5/2^-$, at 4280 MeV and at 4410 MeV.

Therefore, we have predicted eight states, which in our approach are dynamically generated from the meson-baryon interaction. The molecular picture provides important ingredi-

ents on the J^P quantum numbers of these states together with their quark structure and the observation of such states can give support to the molecular nature of these resonances as well as should serve as a good test for the extrapolations used of the chiral unitary approach.

ACKNOWLEDGMENTS

J. M. Dias would like to thank the Brazilian funding agency FAPESP for the financial support under Grant No. 2016/22561–2. V. R. Debastiani wishes to acknowledge the support from the Programa Santiago Grisolia of Generalitat Valenciana (Exp. GRISOLIA/2015/005). This work is also partly supported by the Spanish Ministerio de Economía y Competitividad and European FEDER funds under the contract number FIS2014-57026-REDT, FIS2014-51948-C2-1-P, and FIS2014-51948-C2-2-P, and the Generalitat Valenciana in the program Prometeo II-2014/068. It is also partly supported by the National Natural Science Foundation of China (Grants No. 11475227 and No. 11735003) and the Youth Innovation Promotion Association CAS (No. 2016367).

Appendix A: An example of evaluation of the transition matrix elements for the meson-baryon channels

In what follows we shall illustrate how to obtain the transition amplitudes, represented by the diagram depicted in Fig. 1, using the $\Xi_{cc}\pi \rightarrow \Xi_{cc}\pi$ amplitude as an example. In this case, we have to consider that, in Fig. 1, the initial M_i and final M_f meson will be a pion, while B_i and B_f are the corresponding initial and final baryon, that in this example will be the Ξ_{cc} . The vector meson exchanged V could be a ρ and an ω meson. However, in this particular case, there is no ω meson contribution since this vector meson does not couple to two pions.

Firstly, we have to write the $|\Xi_{cc}\pi\rangle$ in the $I = 1/2$ combination. Remembering the multiplets defined in Eq. (10), we have

$$|\Xi_{cc}\pi (I_3 = 1/2)\rangle = \sqrt{\frac{2}{3}}\Xi_{cc}^+\pi^+ + \sqrt{\frac{1}{3}}\Xi_{cc}^{++}\pi^0. \quad (\text{A1})$$

Therefore, the transition $T_{\Xi_{cc}\pi \rightarrow \Xi_{cc}\pi}$ (before the unitarization of Eq. (14)) will be given evaluating the matrix element $T_{\Xi_{cc}\pi \rightarrow \Xi_{cc}\pi}^{I=1/2} = \langle \Xi_{cc}\pi (I_3 = 1/2) | T | \Xi_{cc}\pi (I_3 = 1/2) \rangle$, that

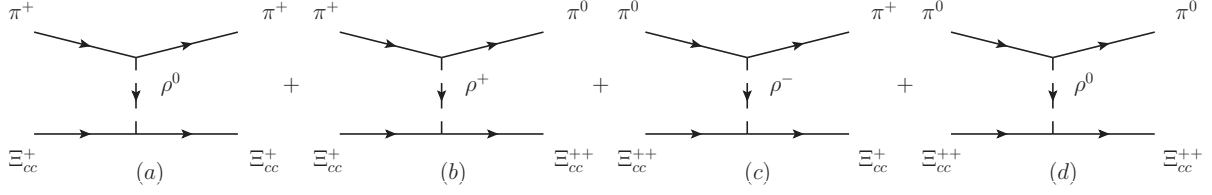


FIG. 2. Diagrams representing the meson-baryon interaction through vector meson exchange for the particular $\Xi_{cc}\pi \rightarrow \Xi_{cc}\pi$ case. In this case, the vector meson exchanged can be a ρ^0 , ρ^+ or ρ^- .

results

$$T_{\Xi_{cc}\pi \rightarrow \Xi_{cc}\pi}^{I=1/2} = \frac{2}{3} t_{\Xi_{cc}^+\pi^+ \rightarrow \Xi_{cc}^+\pi^+} + 2\sqrt{\frac{2}{3}} \sqrt{\frac{1}{3}} t_{\Xi_{cc}^+\pi^+ \rightarrow \Xi_{cc}^+\pi^0} + \frac{1}{3} t_{\Xi_{cc}^+\pi^0 \rightarrow \Xi_{cc}^+\pi^0}. \quad (\text{A2})$$

Thus, the task to get the transition we are interested in involves the calculation of each of the amplitudes appearing in Eq. (A2). The diagrams representing each of them are depicted in Fig. 2. In order to calculate each diagram, we need to obtain all the corresponding upper and lower vertices.

The upper VPP vertices in Fig. 2, are obtained using the Lagrangian in Eq. (1). We get

$$\begin{aligned} -it_{\pi^+ \rightarrow \pi^+} \begin{pmatrix} \rho^0 \\ \omega \end{pmatrix} &= 2igV_\mu(p+p')^\mu \begin{pmatrix} 1/\sqrt{2} \\ 0 \end{pmatrix}, \\ -it_{\pi^+ \rightarrow \pi^0 \rho^+} &= -g \frac{i}{\sqrt{2}} \rho^{+\mu} (p+p')^\mu, \\ -it_{\pi^0 \rightarrow \pi^0} \begin{pmatrix} \rho^0 \\ \omega \end{pmatrix} &= 0. \end{aligned} \quad (\text{A3})$$

The next step focus on the calculation of the VBB vertices. In this case, we shall follow the procedure described in Subsection IIB, in which we have shown how to get the amplitudes using the spin-flavor baryon wave functions. The lower vertices in Fig. 2 involve the Ξ_{cc}^+ and Ξ_{cc}^{++} spin-flavor wave functions, and from Table V we have

$$|\Xi_{cc}^{++}\rangle = |ccu\rangle \otimes |\chi_{MS}\rangle \quad (\text{A4})$$

$$|\Xi_{cc}^+\rangle = |ccd\rangle \otimes |\chi_{MS}\rangle. \quad (\text{A5})$$

Therefore, the vertices $\Xi_{cc}^+\Xi_{cc}^+\rho^0$ and $\Xi_{cc}^+\Xi_{cc}^{++}\rho^+$ are

$$\langle ccd | \frac{g}{\sqrt{2}} (u\bar{u} - d\bar{d}) | ccd \rangle \langle \chi_{MS} | \chi_{MS} \rangle = -\frac{g}{\sqrt{2}}, \quad (\text{A6})$$

$$\langle ccu | g(u\bar{d}) | ccd \rangle \langle \chi_{MS} | \chi_{MS} \rangle = g. \quad (\text{A7})$$

From Eqs. (A3), (A6) and (A7), the diagram in Fig. 2 can be written as

$$\begin{aligned} -iT_{\Xi_{cc}\pi \rightarrow \Xi_{cc}\pi} &= \sum_{\text{diagrams}} (-i)V_{\text{upper}} iG_{\text{prop}} (-i)V_{\text{lower}} \\ &= \frac{2}{3} 2ig \frac{1}{\sqrt{2}} (p_0 + p'_0) \left(\frac{-i}{-M_\rho^2} \right) (i) \left(\frac{-g}{\sqrt{2}} \right) \\ &\quad + 2\sqrt{\frac{2}{3}} \sqrt{\frac{1}{3}} (-i)g \frac{1}{\sqrt{2}} (p_0 + p'_0) \left(\frac{-i}{-M_\rho^2} \right) ig, \end{aligned} \quad (\text{A8})$$

and thus,

$$T_{\Xi_{cc}\pi \rightarrow \Xi_{cc}\pi} = \left(-\frac{4}{3} \right) \frac{1}{4f_\pi^2} (p_0 + p'_0). \quad (\text{A9})$$

V_{upper} and V_{lower} in Eq. (A8) stand for the upper and lower vertices, respectively, while G_{prop} is the propagator related to the vector meson exchanged. In Eq. (A8) we have used $g = M_V/2f_\pi$ to simplify the final expression, given by Eq. (A9). Thus, the coefficient C_{ij} for this transition is $-4/3$, as can be seen in Table VII. Analogously, all the other transition amplitudes can be obtained following the steps shown above.

-
- [1] R. Aaij *et al.* (LHCb Collaboration), Phys. Rev. Lett. **115**, 072001 (2015).
 - [2] R. Aaij *et al.* (LHCb Collaboration), Phys. Rev. Lett. **117**, 082002 (2016).
 - [3] R. Aaij *et al.* (LHCb Collaboration), Phys. Rev. Lett. **117**, 082003 (2016).
 - [4] R. Aaij *et al.* [LHCb Collaboration], Phys. Rev. Lett. **118**, 182001 (2017).
 - [5] R. Aaij *et al.* [LHCb Collaboration], Phys. Rev. Lett. **119**, 112001 (2017).
 - [6] M. Mattson *et al.* [SELEX Collaboration], Phys. Rev. Lett. **89**, 112001 (2002).
 - [7] A. Ocherashvili *et al.* [SELEX Collaboration], Phys. Lett. B **628**, 18 (2005).
 - [8] S. P. Ratti, Nucl. Phys. B, Proc. Suppl. **115**, 33 (2003).
 - [9] B. Aubert *et al.* (BABAR Collaboration), Phys. Rev. D **74**, 011103 (2006).
 - [10] R. Chistov *et al.* (Belle Collaboration), Phys. Rev. Lett. **97**, 162001 (2006).
 - [11] R. Aaij *et al.* (LHCb Collaboration), J. High Energy Phys. **12** (2013) 090.
 - [12] A. De Rujula, H. Georgi and S. L. Glashow, Phys. Rev. D **12**, 147 (1975).
 - [13] D. Ebert, R. N. Faustov, V. O. Galkin and A. P. Martynenko, Phys. Rev. D **66**, 014008 (2002).
 - [14] J. G. Korner, M. Kramer and D. Pirjol, Prog. Part. Nucl. Phys. **33**, 787 (1994).

- [15] R. L. Jaffe and J. E. Kiskis, Phys. Rev. D **13**, 1355 (1976).
- [16] H. X. Chen, W. Chen, X. Liu, Y. R. Liu and S. L. Zhu, Rept. Prog. Phys. **80**, 076201 (2017).
- [17] H. S. Li, L. Meng, Z. W. Liu and S. L. Zhu, Phys. Rev. D **96**, 076011 (2017).
- [18] W. Wang, F. S. Yu and Z. X. Zhao, Eur. Phys. J. C **77**, 781 (2017).
- [19] W. Wang, Z. P. Xing and J. Xu, Eur. Phys. J. C **77**, 800 (2017).
- [20] L. Y. Xiao, Q. F. L and S. L. Zhu, Phys. Rev. D **97**, 074005 (2018).
- [21] H. X. Chen, Q. Mao, W. Chen, X. Liu and S. L. Zhu, Phys. Rev. D **96**, 031501 (2017);
Erratum: [Phys. Rev. D **96**, 119902 (2017)].
- [22] Y. Shimizu and M. Harada, Phys. Rev. D **96**, 094012 (2017).
- [23] Z.-H. Guo, Phys. Rev. D **96**, 074004 (2017).
- [24] J. A. Oller, Ulf-G. Meißner, Phys. Lett. B **500**, 263 (2001).
- [25] D. Jido, J. A. Oller, E. Oset, A. Ramos, U. G. Meißner, Nucl. Phys. A **725**, 181 (2003).
- [26] Ulf-G. Meißner, T. Hyodo, *Pole structure of the $\Lambda(1405)$ region*, in C. Patrignani *et al.* (Particle Data Group), Chin. Phys. C **40**, 100001 (2016).
- [27] C. Garcia-Recio, J. Nieves, E. Ruiz Arriola, M. J. Vicente Vacas, Phys. Rev. D **67**, 076009 (2003).
- [28] E. Oset and A. Ramos, Eur. Phys. J. A **44**, 445 (2010).
- [29] S. Sarkar, B. X. Sun, E. Oset and M. J. Vicente Vacas, Eur. Phys. J. A **44**, 431 (2010).
- [30] M. Bando, T. Kugo and K. Yamawaki, Phys. Rept. **164**, 217 (1988).
- [31] M. Harada and K. Yamawaki, Phys. Rept. **381**, 1 (2003).
- [32] Ulf-G. Meißner, Phys. Rept. **161**, 213 (1988).
- [33] W. H. Liang, T. Uchino, C. W. Xiao and E. Oset, Eur. Phys. J. A **51**, 16 (2015).
- [34] T. Uchino, W. H. Liang and E. Oset, Eur. Phys. J. A **52**, 43 (2016).
- [35] J. Hofmann and M. F. M. Lutz, Nucl. Phys. A **763**, 90 (2005).
- [36] T. Mizutani and A. Ramos, Phys. Rev. C **74**, 065201 (2006).
- [37] V. R. Debastiani, J. M. Dias, W. H. Liang and E. Oset, Phys. Rev. D in print, [arXiv:1710.04231](https://arxiv.org/abs/1710.04231) [hep-ph].
- [38] G. Montana, A. Feijoo and A. Ramos, Eur. Phys. J. A **54**, 64 (2018).
- [39] O. Romanets, L. Tolos, C. Garcia-Recio, J. Nieves, L. L. Salcedo and R. G. E. Timmermans, Phys. Rev. D **85**, 114032 (2012).
- [40] J. Nieves, R. Pavao and L. Tolos, Eur. Phys. J. C **78**, no. 2, 114 (2018).

- [41] W. H. Liang, J. M. Dias, V. R. Debastiani and E. Oset, Nucl. Phys. B **930**, 524 (2018).
- [42] C. Albertus, E. Hernandez and J. Nieves, Phys. Lett. B **683**, 21 (2010).
- [43] C. Patrignani *et al.* (Particle Data Group), Chin. Phys. C **40**, 100001 (2016).
- [44] W. H. Liang, C. W. Xiao, and E. Oset, Phys. Rev. D **89**, 054023 (2014).
- [45] S. Sakai, L. Roca and E. Oset, Phys. Rev. D **96**, 054023 (2017).
- [46] E. Oset, A. Ramos and C. Bennhold, Phys. Lett. B **527**, 99 (2002); Erratum: [Phys. Lett. B **530**, 260 (2002)].
- [47] E. Oset and A. Ramos, Nucl. Phys. A **635**, 99 (1998).
- [48] J. A. Oller and E. Oset, Nucl. Phys. A **620**, 438 (1997); Erratum-ibid. A **652**, 407 (1999).
- [49] J. J. Wu and B. S. Zou, Phys. Lett. B **709**, 70 (2012).
- [50] A. Ozpineci, C. W. Xiao, and E. Oset, Phys. Rev. D **88**, 034018 (2013).
- [51] J. X. Lu, Y. Zhou, H. X. Chen, J. J. Xie, and L. S. Geng, Phys. Rev. D **92**, 014036 (2015).
- [52] E. J. Garzon and E. Oset, Eur. Phys. J. A **48**, 5 (2012).
- [53] D. Gamermann, J. Nieves, E. Oset, and E. Ruiz Arriola, Phys. Rev. D **81**, 014029 (2010).